SANDIA REPORT
SAND2020-12165
Printed November 2020

Sandia National Laboratories

Coherent Processing of Up/Down Linear Frequency Modulated Chirps

Armin W Doerry

Prepared by
Sandia National Laboratories
Albuquerque, New Mexico
87185 and Livermore,
California 94550

Issued by Sandia National Laboratories, operated for the United States Department of Energy by National Technology & Engineering Solutions of Sandia, LLC.

Available to DOE and DOE contractors from
U.S. Department of Energy
Office of Scientific and Technical Information
P.O. Box 62
Oak Ridge, TN 37831

Telephone: (865) 576-8401
Facsimile: (865) 576-5728
E-Mail: reports@osti.gov
Online ordering: http://www.osti.gov/scitech

Available to the public from
U.S. Department of Commerce
National Technical Information Service
5301 Shawnee Rd
Alexandria, VA 22312

Telephone: (800) 553-6847
Facsimile: (703) 605-6900
E-Mail: orders@ntis.gov
Online order: https://classic.ntis.gov/help/order-methods/

Coherent Processing of Up/Down Linear Frequency Modulated Chirps

Armin W Doerry

Abstract

A useful and popular waveform for high-performance radar systems is the Linear Frequency Modulated (LFM) chirp. The chirp may have a positive frequency slope with time (up-chirp) or a negative frequency slope with time (down-chirp). There is no inherent advantage to one with respect to the other, except that the receiver needs to be matched to the proper waveform. However, if up-chirps and down-chirps are employed on different pulses in the same Coherent Processing Interval (CPI), then care must be taken to maintain coherence in the range-compressed echo signals. We present the mathematics for doing so, for both correlation processing and stretch processing.

Acknowledgements

This report was the result of an unfunded research and development activity.

A special thanks to my colleague Doug Bickel for being an invaluable sounding board for this work and many others.

Contents

List of Figures

Acronyms and Definitions

1-D, 2-D, 3-D	1-, 2-, 3-Dimesional
ADC	Analog to Digital Converter
CPI	Coherent Processing Interval
DC	Direct Current, a.k.a. zero-frequency
DFT	Discrete Fourier Transform
DDS	Direct Digital Synthesis/Synthesizer
DWS	Digital Waveform Synthesizer
FFT	Fast Fourier Transform
IF	Intermediate Frequency
IDFT	Inverse DFT
ISR	Intelligence, Surveillance, and Reconnaissance
IPR	Impulse Response
LFM	Linear Frequency Modulated
RVPE	Residual Video Phase Error
T&C	Timing and Control
WFS	Waveform Synthesizer

Foreword

This report details the results of an academic study. It does not presently exemplify any modes, methodologies, or techniques employed by any operational system known to the author.

Classification

The specific mathematics and algorithms presented herein do not bear any release restrictions or distribution limitations.

This report formalizes preexisting informal notes and other documentation on the subject matter herein.

This report has been reviewed and approved to be Unclassified – Unlimited Release.

Author Contact Information

Armin Doerry awdoerr@sandia.gov 505-845-8165

1 Introduction

Typical high-performance radar systems used for Intelligence, Surveillance, and Reconnaissance (ISR) employ waveform modulation to enhance the bandwidth, and hence range-resolution, of the radar. A common waveform is the Linear Frequency Modulated (LFM) chirp.[1] These waveforms can be generated with high-fidelity and precision, using Direct Digital Synthesis (DDS), in Digital Waveform Synthesizers (DWS, or WFS).[2]

In general, there is no processing advantage for an LFM chirp having a positive frequency slope with time, or a negative frequency slope with time; the slope being the chirp rate. Both offer identical radar performance, albeit need to be processed with deference to their precise nature of the chirp rate. Generally, however, radar systems are designed and operated so that any single Coherent Processing Interval (CPI), or synthetic aperture, will have the same chirp-rate sign for the entirety of the CPI or synthetic aperture.

It has been proposed that there might be some advantage by alternating in some manner the chirp-rate sign for different pulses in a common CPI. The chirp-rate sign might be altered in some periodic manner, or even in some random, or pseudo-random manner. The advantages have been suggested with respect to ambiguous range mitigation, or other interference mitigation, with the expectation that a wrong-sign chirp from an ambiguous range will be rejected to a large degree by a matched filter or correlator. An advantage has also been suggested for incidents of spoofing or other interference mitigation.

Aspects of manipulating chirp rates across pulses have been previously reported. For example:

> Mittermayer and Martínez explore "up and down chirp modulation on point and extended target signals." [3]
>
> Wang "investigates a scheme for designing chirp modulation diversity waveforms" that includes up and down chirps.[4]
>
> Lulu and Mobasseri discuss the more general case of "a pulse train modeled after chirplet chains where the basic elements of the waveform are contiguous linear chirps of arbitrary chirp rates and offset frequencies without using frequency coding." [5]

This listing is not comprehensive, and many other publications address this topic as well.

In any case, we wish to further explore herein the question "How can we coherently combine radar echoes generated from chirps differing in their chirp-rate sign, i.e. up and down chirps?" Such coherently combining of these chirps is necessary for, say, Doppler processing.

This report examines the impact of chirp-rate sign on the processed output of a range-compressed signal. We examine herein both correlation processing and stretch processing. We furthermore examine the processing steps necessary to properly coherently combine signals generated with different chirp-rate signs.

“If at first you don't succeed, try reading the instructions!”
-- Harry Stine, 1962

2 LFM Chirp Echo

Consider a transmitted Linear Frequency Modulated (LFM) chirp waveform, described by

$$X_T(t,n) = A_T \,\mathrm{rect}\left(\frac{t-t_n}{T}\right)\cos\left(\phi_T + \omega_T(t-t_n) + q\frac{\gamma_T}{2}(t-t_n)^2\right), \tag{1}$$

where

A_T = amplitude of transmitted waveform,
t_n = reference time of the nth pulse,
T = transmitted pulse width,
ϕ_T = reference phase of the transmitted waveform,
ω_T = reference frequency of the transmitted waveform,
γ_T = reference chirp rate of the transmitted waveform, and
$q \in \{-1,+1\}$, defining the sign of the chirp rate, (2)

and the function

$$\mathrm{rect}(z) = \begin{cases} 1 & |z| \le 1/2 \\ 0 & else \end{cases}. \tag{3}$$

Without loss of generality, we will assume $\gamma_T > 0$. The net chirp direction is then given by q. We will refer to chirp with a positive q as an "up-chirp," and one with a negative q as a "down-chirp."

The received radar echo waveform from an ideal point reflector may be written as

$$X_R(t,n) = A_R \,\mathrm{rect}\left(\frac{t-t_n-t_{s,n}}{T}\right)\cos\left(\phi_T + \omega_T(t-t_n-t_{s,n}) + q\frac{\gamma_T}{2}(t-t_n-t_{s,n})^2\right), \tag{4}$$

where

A_R = amplitude of received waveform,
$t_{s,n}$ = echo delay time of the point reflector for the nth pulse. (5)

We mix this signal with a Local Oscillator (LO) waveform effectively of the form

$$X_{LO}(t,n) = 2\,\mathrm{rect}\left(\frac{t-t_n-t_{m,n}}{T_L}\right)\exp\left\{-j\left(\phi_L + \omega_L(t-t_n-t_{m,n}) + q\frac{\gamma_L}{2}(t-t_n-t_{m,n})^2\right)\right\}, \tag{6}$$

where the LO waveform parameters are

$t_{m,n}$ = LO waveform reference time for the nth pulse,
T_L = LO pulse width,
ϕ_L = reference phase of the transmitted waveform,
ω_L = reference frequency of the transmitted waveform, and
γ_L = reference chirp rate of the transmitted waveform. (7)

Demodulating this echo signal to baseband yields the video signal expression

$$X_V(t,n) = \left[\begin{array}{l} A_R \,\mathrm{rect}\left(\dfrac{t - t_n - t_{s,n}}{T} \right) \mathrm{rect}\left(\dfrac{t - t_n - t_{m,n}}{T_L} \right) \\ \times \exp\left\{ j \left(\begin{array}{l} \phi_T + \omega_T \left(t - t_n - t_{s,n} \right) + q \dfrac{\gamma_T}{2} \left(t - t_n - t_{s,n} \right)^2 \\ -\phi_L - \omega_L \left(t - t_n - t_{m,n} \right) - q \dfrac{\gamma_L}{2} \left(t - t_n - t_{m,n} \right)^2 \end{array} \right) \right\} \end{array} \right], \tag{8}$$

which we rearrange to

$$X_V(t,n) = \left[\begin{array}{l} A_R \,\mathrm{rect}\left(\dfrac{t - t_n - t_{s,n}}{T} \right) \mathrm{rect}\left(\dfrac{t - t_n - t_{m,n}}{T_L} \right) \\ \times \exp\left\{ j \left(\begin{array}{l} \phi_T - \phi_L \\ +\omega_T \left(t - t_n - t_{s,n} \right) - \omega_L \left(t - t_n - t_{m,n} \right) \\ +q \dfrac{\gamma_T}{2} \left(t - t_n - t_{s,n} \right)^2 - q \dfrac{\gamma_L}{2} \left(t - t_n - t_{m,n} \right)^2 \end{array} \right) \right\} \end{array} \right]. \tag{9}$$

At this point without loss to the point we are investigating, we will make the following assumptions,

$\phi_L = \phi_T$, and
$\omega_L = \omega_T$, (10)

which allows us the simplification

$$X_V(t,n) = \left[\begin{array}{l} A_R \,\mathrm{rect}\left(\dfrac{t - t_n - t_{s,n}}{T} \right) \mathrm{rect}\left(\dfrac{t - t_n - t_{m,n}}{T_L} \right) \\ \times \exp\left\{ j \left(\begin{array}{l} \omega_T \left(t_{m,n} - t_{s,n} \right) \\ + q \dfrac{\gamma_T}{2} \left(t - t_n - t_{s,n} \right)^2 - q \dfrac{\gamma_L}{2} \left(t - t_n - t_{m,n} \right)^2 \end{array} \right) \right\} \end{array} \right]. \tag{11}$$

The value which we will assume for the LO chirp rate γ_L will depend on the subsequent range-compression processing strategy; whether we employ correlation processing or stretch processing.[6]

We will ignore for now any Doppler "within" the pulse, manifesting as an intra-pulse time-dependence of the delay term $t_{s,n}$. This is also sometimes referred to as the "stop-and-go" assumption, where the radar geometry is presumed frozen for the duration of the pulse, and changes only between pulses. The relevant Doppler term for us will be the inter-pulse phase change due to an inter-pulse change in $t_{s,n}$. This is principally a function of the first phase term, $\omega_T \left(t_{m,n} - t_{s,n} \right)$.

2.1 Correlation Processing

While virtually all radar coherent data processing attempts to implement a matched-filter to pixel locations, velocities, and other attributes of interest, the term "correlation processing" is usually reserved for range-compressing digital echo data for which the chirp nature has not yet been removed.

Consequently, the baseband video signal may be modelled with Eq. (11), where the LFM chirp rate is not compensated by the LO, implying that

$$\gamma_L = 0 . \tag{12}$$

Furthermore, the analog signal is digitized by the Analog-to-Digital Converter (ADC) by sampling at times

$$\left(t - t_n - t_{m,n} \right) = T_s i , \tag{13}$$

where

$$\begin{array}{l} T_s = \text{ADC sampling period within a pulse echo, and} \\ i = \text{fast-time sample index, with } -I/2 \le i < I/2 . \end{array} \tag{14}$$

The definition of fast-time index *i* with these limits is a convenience for our development. It allows for cleaner derivations, and does not diminish the salient points we wish to discuss in this report.

The baseband video data is then described by

$$X_V(i,n) = \left[\begin{array}{l} A_R \,\mathrm{rect}\left(\dfrac{T_s i + t_{m,n} - t_{s,n}}{T} \right) \mathrm{rect}\left(\dfrac{T_s i}{T_L} \right) \\ \times \exp\left\{ j \left(\begin{array}{l} \omega_T \left(t_{m,n} - t_{s,n} \right) \\ + q \dfrac{\gamma_T}{2} \left(T_s i + t_{m,n} - t_{s,n} \right)^2 \end{array} \right) \right\} \end{array} \right]. \tag{15}$$

With malice aforethought, we make some additional observations as follows.

- The LO pulsewidth T_L need not be wider than the data we wish to collect. Consequently, we may set

$$T_L = T_s I \,. \tag{16}$$

- The time difference $\left(t_{s,n} - t_{m,n} \right)$ is just the relative delay of the actual echo time from the reference echo time. We may simplify our expression by defining this relative delay as

$$\left(t_{s,n} - t_{m,n} \right) = \tau_{sm,n} \,. \tag{17}$$

- We are only really interested in target echo delay times where the response from the range of interest fits entirely in the baseband video data set. This means that for this case $T < T_L$. This also means that we may allow

$$\mathrm{rect}\left(\frac{T_s i + t_{m,n} - t_{s,n}}{T} \right) \mathrm{rect}\left(\frac{T_s i}{T_L} \right) = \mathrm{rect}\left(\frac{T_s i - \tau_{sm,n}}{T} \right). \tag{18}$$

The baseband video data can then be described by the simplified expression

$$X_V(i,n) = \left[\begin{array}{l} A_R e^{-j\omega_T \tau_{sm,n}} \\ \times \mathrm{rect}\left(\dfrac{T_s i - \tau_{sm,n}}{T} \right) e^{jq\frac{\gamma_T}{2}\left(T_s i - \tau_{sm,n} \right)^2} \end{array} \right]. \tag{19}$$

In this expression, the first line contains the target echo amplitude, and the Doppler phase term. The second line is a baseband LFM chirp that is centered on the relative delay $\tau_{sm,n}$. To precisely find this relative delay requires correlating this signal against a kernel, or set of kernels, to find the best fit. The output of the correlator may be described by

$$Y(u,n) = \sum_{k=-K/2}^{K/2-1} g^*(k,n)\, X_V(k+u,n), \tag{20}$$

where the correlation kernel is defined by

$$g(k,n) = \text{rect}\left(\frac{T_s k}{T}\right) e^{jq\frac{\gamma_T}{2}(T_s k)^2}, \tag{21}$$

where

$$T_s K = T\,. \tag{22}$$

For this development we are ignoring any data tapering for sidelobe control.

Putting all this together yields

$$Y(u,n) = \left[\begin{array}{l} A_R e^{-j\omega_T \tau_{sm,n}} \\ \times \sum_{k=-K/2}^{K/2-1} \text{rect}\left(\frac{T_s k}{T}\right) \text{rect}\left(\frac{T_s k + T_s u - \tau_{sm,n}}{T}\right) e^{j\left[\begin{array}{l} q\frac{\gamma_T}{2}\left(T_s k + T_s u - \tau_{sm,n}\right)^2 \\ -q\frac{\gamma_T}{2}(T_s k)^2 \end{array}\right]} \end{array}\right]. \tag{23}$$

This may be simplified somewhat to

$$Y(u,n) = \left[\begin{array}{l} A_R e^{-j\omega_T \tau_{sm,n}} e^{jq\frac{\gamma_T}{2}\left(T_s u - \tau_{sm,n}\right)^2} \\ \times \sum_{k=-K/2}^{K/2-1} \text{rect}\left(\frac{T_s k}{T}\right) \text{rect}\left(\frac{T_s k + T_s u - \tau_{sm,n}}{T}\right) e^{jq\gamma_T\left(T_s u - \tau_{sm,n}\right)(T_s k)} \end{array}\right]. \tag{24}$$

The principle of stationary phase suggests that for us the meaningful response is in the neighborhood of $T_s u \approx \tau_{sm,n}$. In this neighborhood, we may simplify Eq. (24) further to

$$Y(u,n) \approx A_R e^{-j\omega_T \tau_{sm,n}} e^{jq\frac{\gamma_T}{2}\left(T_s u - \tau_{sm,n}\right)^2} \sum_{k=-K/2}^{K/2-1} e^{jq\gamma_T\left(T_s u - \tau_{sm,n}\right)(T_s k)}\,. \tag{25}$$

The closed-form solution to this is

$$Y(u,n) \approx K A_R \left(\frac{\sin\left(\frac{\gamma_T}{2}\left(T_s u - \tau_{sm,n}\right) T_s K\right)}{K \sin\left(\frac{\gamma_T}{2}\left(T_s u - \tau_{sm,n}\right) T_s\right)}\right) \left[\begin{array}{l} e^{jq\frac{\gamma_T}{2}\left[\left(T_s u - \tau_{sm,n}\right)^2 - \left(T_s u - \tau_{sm,n}\right) T_s\right]} \\ \times e^{-j\omega_T \tau_{sm,n}} \end{array}\right]. \tag{26}$$

This may further be approximated in the region of $T_s u \approx \tau_{sm,n}$ as

$$Y(u,n) \approx KA_R \operatorname{sinc}\left(\frac{\gamma_T}{2\pi} T_s K\left(T_s u - \tau_{sm,n}\right)\right)\left[\begin{array}{l} e^{jq\frac{\gamma_T}{2}\left[\left(T_s u-\tau_{sm,n}\right)^2-\left(T_s u-\tau_{sm,n}\right)T_s\right]} \\ \quad \times e^{-j\omega_T \tau_{sm,n}} \end{array}\right], \tag{27}$$

where we identify the function

$$\operatorname{sinc}(z) = \frac{\sin(\pi z)}{\pi z}. \tag{28}$$

We may define the temporal resolution of Eq. (27) as the distance (in time) between peak and first null, namely when

$$\left|\frac{\gamma_T}{2\pi} T_s K\left(T_s u - \tau_{sm,n}\right)\right|_{\substack{u=0 \\ \tau_{sm,n}=\rho_t}} = 1. \tag{29}$$

This may be solved to yield

$$\rho_t = \frac{1}{\frac{\gamma_T}{2\pi} T_s K} = \frac{1}{B_c} = \text{time resolution}, \tag{30}$$

where we define

$$B_c = \frac{\gamma_T}{2\pi} T_s K = \text{the LFM chirp waveform bandwidth}. \tag{31}$$

The range resolution can be calculated as the familiar

$$\rho_r = \frac{c}{2}\rho_t = \frac{c}{2B_c} = \text{range resolution}. \tag{32}$$

We turn our attention now to the first phase term in Eq. (27), and morph it to the equivalent expression

$$\frac{\gamma_T}{2}\left[\left(T_s u - \tau_{sm,n}\right)^2 - \left(T_s u - \tau_{sm,n}\right)T_s\right] = \pi B_c T_s \left[\frac{\left(u - \frac{\tau_{sm,n}}{T_s}\right)^2 - \left(u - \frac{\tau_{sm,n}}{T_s}\right)}{K}\right]. \tag{33}$$

We observe from this new expression that proper sampling of the signal stipulates that $B_c T_s < 1$. Furthermore, the expression in the square brackets on the right-hand side of Eq. (33) will also be much less than one anywhere near the peak, where $u = \tau_{sm,n} / T_s$. Taken together, this renders this phase term as pretty much inconsequential, and Eq. (27) may be acceptably approximated as

$$Y(u,n) \approx KA_R \operatorname{sinc}\left(\frac{\gamma_T}{2\pi} T_s K \left(T_s u - \tau_{sm,n} \right) \right) e^{-j\omega_T \tau_{sm,n}} . \tag{34}$$

Of particular note is that any dependence on chirp-rate sign, q, has been eliminated in Eq. (34).

A more thorough discussion of digital correlation of chirp signals is given in an earlier report.[7]

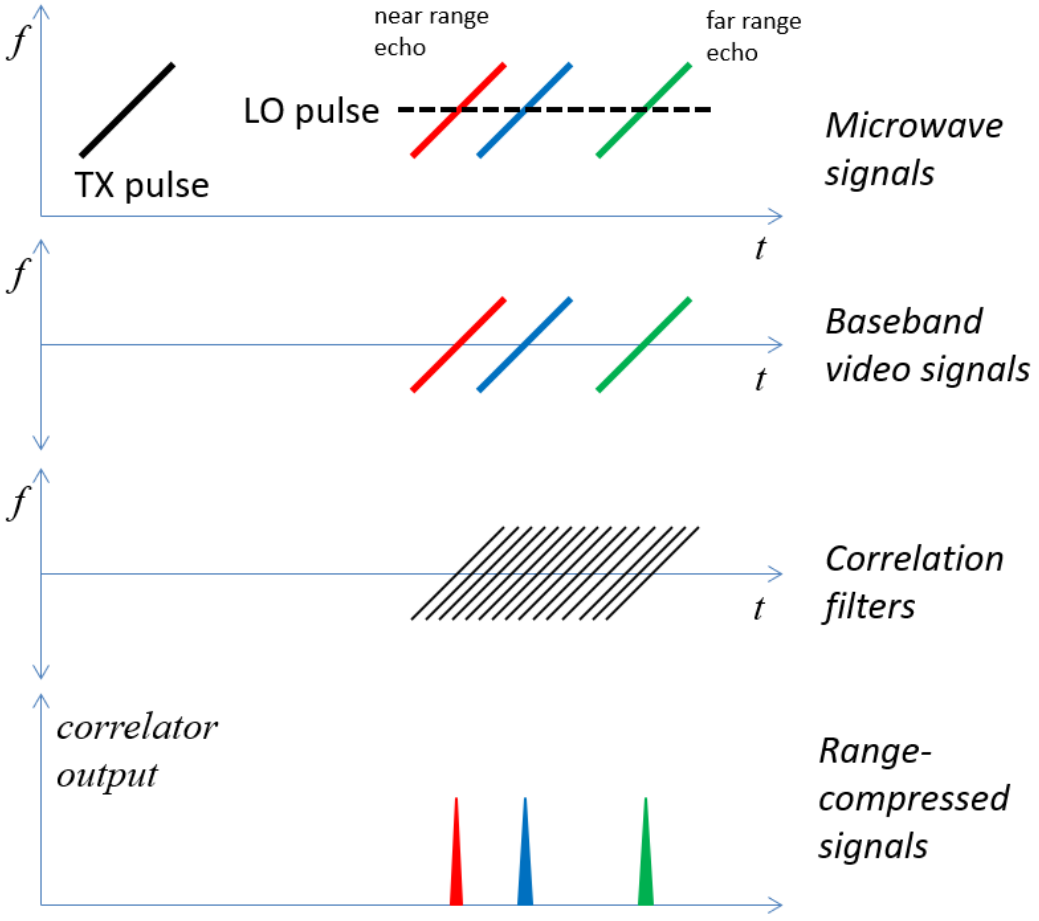

Figure 1. Pulse compression via correlation filters is indicated when the range swath is a large fraction (or larger) of the TX pulse width, or for coarser range resolutions. Note that the baseband video signal bandwidth is the same as the microwave signal bandwidth. This model applies to other waveforms, too.

2.2 Stretch Processing

Stretch processing is unique to the LFM chirp waveform; making use of the linear frequency with time relationship. That is, for an LFM chirp, a time offset is essentially (albeit not perfectly exactly) equivalent to a frequency offset.

The matched-filter operation is typically implemented in two stages:

1. An analog mixing of the return echoes with an LO chirp reference signal, called "dechirping," followed by

2. A digital correlation against different frequencies, where frequency offset is proportional to time offset due to the nature of the LFM chirp. This digital correlation against different frequencies is typically implemented with a Discrete Fourier Transform (DFT), or more commonly its Fast Fourier Transform (FFT) counterpart.

Consequently, the baseband video signal may now be modelled with Eq. (11), but where the LFM chirp rate is compensated by the LO, implying that

$$\gamma_L = \gamma_T \,. \tag{35}$$

Consequently Eq. (11) becomes

$$X_V\left(t,n\right) = \left[\begin{array}{l} A_R \,\mathrm{rect}\left(\dfrac{t-t_n-t_{s,n}}{T}\right)\mathrm{rect}\left(\dfrac{t-t_n-t_{m,n}}{T_L}\right) \\ \times \exp\left\{ j\left(\begin{array}{l} \omega_T\left(t_{m,n}-t_{s,n}\right) \\ +q\dfrac{\gamma_T}{2}\left(t-t_n-t_{s,n}\right)^2 - q\dfrac{\gamma_T}{2}\left(t-t_n-t_{m,n}\right)^2 \end{array} \right) \right\} \end{array}\right], \tag{36}$$

which can be expanded and simplified to

$$X_V\left(t,n\right) = \left[\begin{array}{l} A_R \,\mathrm{rect}\left(\dfrac{t-t_n-t_{s,n}}{T}\right)\mathrm{rect}\left(\dfrac{t-t_n-t_{m,n}}{T_L}\right) \\ \times \exp\left\{ j\left(\begin{array}{l} \omega_T\left(t_{m,n}-t_{s,n}\right) \\ +q\gamma_T\left(t_{m,n}-t_{s,n}\right)\left(t-t_n-t_{m,n}\right) \\ +q\dfrac{\gamma_T}{2}\left(t_{m,n}-t_{s,n}\right)^2 \end{array} \right) \right\} \end{array}\right]. \tag{37}$$

Employing the sampling of Eq. (13), and the simplification of Eq. (17), yields

$$X_V(i,n) = A_R \,\mathrm{rect}\left(\frac{T_s i - \tau_{sm,n}}{T}\right)\mathrm{rect}\left(\frac{T_s i}{T_L}\right)\exp\left\{ j\begin{pmatrix} -\omega_T \tau_{sm,n} \\ -q\gamma_T \tau_{sm,n} T_s i \\ +q\frac{\gamma_T}{2}\tau_{sm,n}{}^2 \end{pmatrix}\right\}. \tag{38}$$

For this report we will make an assumption that I is odd. This is purely a convenience for the following development, allowing us to focus on concepts rather than indexing details. Consequently, we stipulate

$$-(I-1)/2 \;\le\; i \;\le\; (I-1)/2\,. \tag{39}$$

In addition, we make some further observations.

- The LO pulsewidth T_L need not be wider than the data we wish to collect. Consequently, as with correlation processing, we may set

$$T_L = T_s I\,. \tag{40}$$

- We observe that the envelope of the echo signal is also target-range dependent; depends on relative delay $\tau_{sm,n}$. Consequently, if we wish all fast-time samples i to contain data from all relative delays $\tau_{sm,n}$ of interest, then we will require an extension of the transmitted pulsewidth T such that

$$T > T_s I + 2\max\left|\tau_{sm,n}\right|. \tag{41}$$

  This is well-known about stretch processing. Consequently, this leads to the condition

$$\mathrm{rect}\left(\frac{T_s i - \tau_{sm,n}}{T}\right)\mathrm{rect}\left(\frac{T_s i}{T_L}\right) = \mathrm{rect}\left(\frac{T_s i}{T_L}\right), \tag{42}$$

  which is essentially "1" for all fast-time indices i.

These observations allow us to express Eq. (38) as simply

$$X_V(i,n) = A_R \exp\left\{ j\left(-\omega_T \tau_{sm,n} - \; q\gamma_T \tau_{sm,n} T_s i \; + \; q\frac{\gamma_T}{2}\tau_{sm,n}{}^2 \right)\right\}. \tag{43}$$

We note that the first phase term is the Doppler term, as with correlation processing. The second phase term is the frequency term that is proportional to target range offset.

The third phase term in Eq. (43) is unique to stretch processing, and is called the Residual Video Phase Error (RVPE). It is sometimes called a "skew" term. Techniques exist to compensate this error term, and implementing this removal or compensation is sometimes called "deskewing."

Rearranging terms somewhat allow us to express Eq. (43) as

$$X_V\left(i,n\right) = A_R e^{-j\omega_T \tau_{sm,n}} e^{jq\frac{\gamma_T}{2}\tau_{sm,n}^{\ 2}} e^{-jq\gamma_T \tau_{sm,n} T_s i}. \tag{44}$$

Given this expression, and the limits of fast-time index i, we process this with a DFT as

$$Y\left(u,n\right) = \sum_{i=-\left(I-1\right)/2}^{\left(I-1\right)/2} X_V\left(i,n\right) e^{-j2\pi\frac{u}{U}i}, \text{ for } -\left(U-1\right)/2 \le u < \left(U-1\right)/2, \tag{45}$$

which we expand as

$$Y\left(u,n\right) = A_R e^{-j\omega_T \tau_{sm,n}} e^{jq\frac{\gamma_T}{2}\tau_{sm,n}^{\ 2}} \sum_{i=-\left(I-1\right)/2}^{\left(I-1\right)/2} e^{-jq\gamma_T \tau_{sm,n} T_s i} e^{-j2\pi\frac{u}{U}i}. \tag{46}$$

Typically, $U = I$, and we shall assume so for the following development.

As with correlation processing, for this development we are ignoring any data tapering for sidelobe control. The closed-form solution to this is

$$Y\left(u,n\right) = IA_R \left(\frac{\sin\left(\pi \frac{I}{2\pi}\left(q\gamma_T \tau_{sm,n} T_s + 2\pi\frac{u}{I}\right)\right)}{I\sin\left(\pi \frac{1}{2\pi}\left(q\gamma_T \tau_{sm,n} T_s + 2\pi\frac{u}{I}\right)\right)} \right) e^{-j\omega_T \tau_{sm,n}} e^{jq\frac{\gamma_T}{2}\tau_{sm,n}^{\ 2}}. \tag{47}$$

This may further be approximated in the region of the mainlobe as

$$Y\left(u,n\right) \approx IA_R \,\mathrm{sinc}\left(\frac{\gamma_T}{2\pi} T_s I \left(\frac{qu}{\frac{\gamma_T}{2\pi} T_s I} + \tau_{sm,n} \right) \right) e^{-j\omega_T \tau_{sm,n}} e^{jq\frac{\gamma_T}{2}\tau_{sm,n}^{\ 2}}. \tag{48}$$

As with correlation processing, we may evaluate the time resolution by equating

$$\left| \frac{\gamma_T}{2\pi} T_s I \left(\frac{qu}{\frac{\gamma_T}{2\pi} T_s I} + \tau_{sm,n} \right) \right|_{\substack{u=0 \\ \tau_{sm,n}=\rho_t}} = 1, \tag{49}$$

and solving for

$$\rho_t = \frac{1}{\frac{\gamma_T}{2\pi} T_S I} = \frac{1}{B_{eff}} \text{ = time resolution,} \tag{50}$$

where we define

$$B_{eff} = \frac{\gamma_T}{2\pi} T_S I \text{ = the LFM chirp waveform bandwidth present in the data.} \tag{51}$$

From Eq. (41), we recall that $T > T_S I$, meaning that the pulsewidth of the transmitted pulse is wider than the data record for that pulse. Since chirp rate is constant, this also means that the transmitted chirp bandwidth is wider than the bandwidth of the radar echoes represented in the data. That is

$B_c > B_{eff}$, where

$$B_c = \frac{\gamma_T}{2\pi} T \text{ = transmitted chirp bandwidth.} \tag{52}$$

The range resolution is based on the effective bandwidth as it manifests in the data, and can be calculated as the familiar

$$\rho_r = \frac{c}{2} \rho_t = \frac{c}{2B_{eff}} \text{ = range resolution.} \tag{53}$$

Returning to Eq. (48), we observe that chirp rate sign q appears in two places.

First, it appears in the argument of the sinc function, and has the effect of reversing the direction of index u. We state without elaboration for now that $u = 0$ describes the zero-frequency, or DC point, regardless of q.

Second, it appears in the RVPE term. The magnitude of this phase may be calculated as

$$\left| q \frac{\gamma_T}{2} \tau_{sm,n}{}^2 \right| = \pi \frac{B_{eff}}{T_S I} \tau_{sm,n}{}^2 . \tag{54}$$

A simple example shows the significance of this term. Consider a relative range offset of 100 m, with a chirp rate of 500 MHz over 20 μs; not at all unusual for a high-performance radar system. This corresponds to a phase of about 35 radians, which may be +/– depending on q. The implication is that although this is a phase term in the final range-compressed data, it can be rather large, and can't be ignored if q changes.

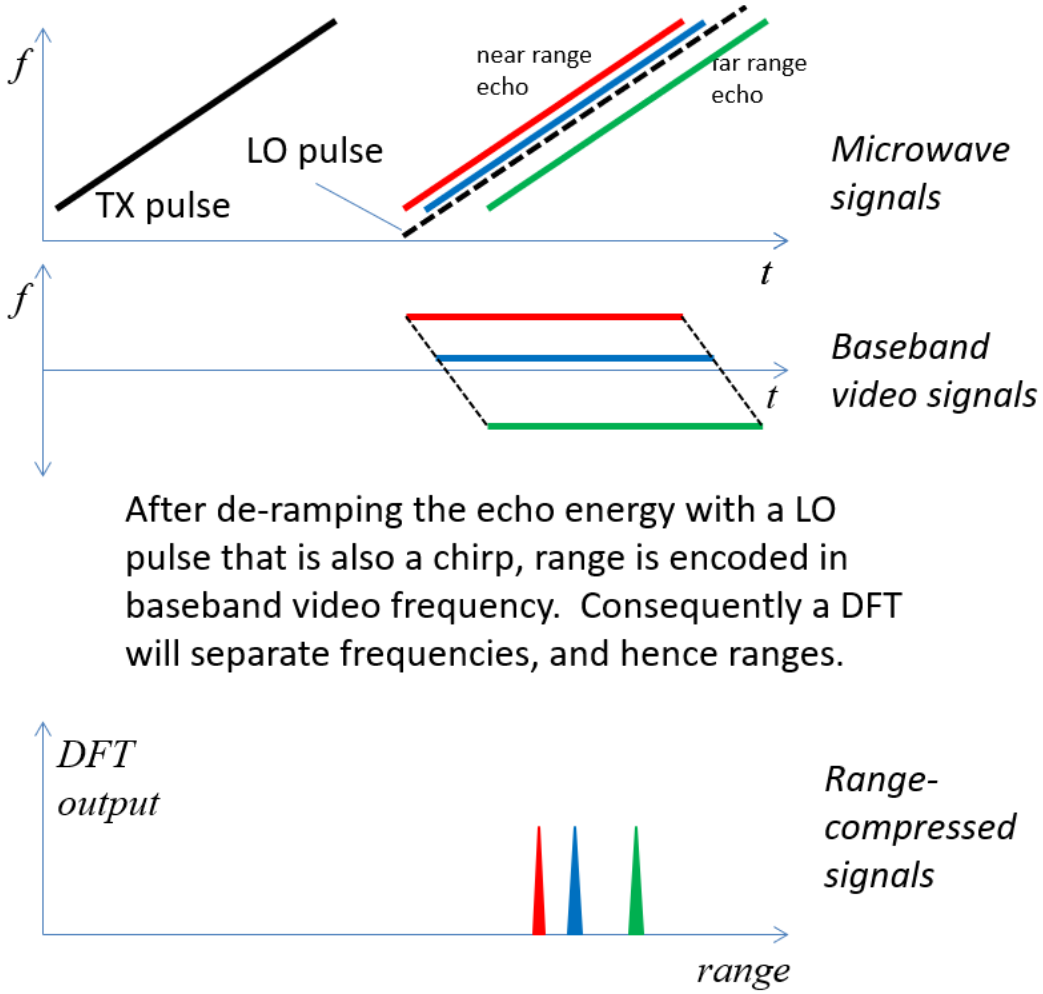

Figure 2. Pulse compression via stretch processing is indicated when the range swath is a small fraction of the TX pulse width, or for finer range resolutions. Note that the baseband video signal bandwidth is less than the microwave signal bandwidth. Stretch processing generally assumes LFM chirp waveforms.

3 Processing a Chirp with the Wrong Sign

Since one of the reasons for endowing a CPI with pulses that have both up and down chirps is to mitigate responses from echoes with the wrong chirp-rate sign.

We wish now to contrast processing a chirp echo against a reference chirp, both with the correct chirp-rate sign, and the wrong chirp-rate sign.

Since this exercise is meant to be illustrative, we will concern ourselves with continuous-time baseband signals. We begin with Eq. (11), adopt the simplification of Eq. (17), and assume correlation processing of the continuous-time baseband signal. Our new relative time variable becomes

$$\left(t - t_n - t_{m,n}\right) = t' . \tag{55}$$

Consequently, let our echo return signal be specified as

$$X_V\left(t,n\right) = \left[\begin{array}{l} A_R \,\mathrm{rect}\left(\dfrac{t' - \tau_{sm,n}}{T}\right) \\ \times \exp\left\{ j\left(-\omega_T \tau_{sm,n} + \dfrac{\gamma_T}{2}\left(t' - \tau_{sm,n}\right)^2 \right) \right\} \end{array}\right] . \tag{56}$$

The correlation kernel is given as

$$g\left(t,n\right) = \mathrm{rect}\left(\frac{t'}{T}\right) e^{jq\frac{\gamma_T}{2}\left(t'\right)^2} . \tag{57}$$

The correlation operation is given generically by

$$y\left(t',n\right) = \mathrm{xcorr}\left(g\left(t',n\right), X_V\left(t',n\right)\right) = \int_{-\infty}^{\infty} g^*\left(u,n\right) X_V\left(u + t',n\right) du . \tag{58}$$

The parameter *u* here is simply the variable of integration.

Applying this to our echo signal and kernel yields

$$y\left(t',n\right) = \int_{-\infty}^{\infty} \left[\mathrm{rect}\left(\frac{u}{T}\right) e^{jq\frac{\gamma_T}{2}\left(u\right)^2} \right]^* \left[\begin{array}{l} A_R \,\mathrm{rect}\left(\dfrac{t' + u - \tau_{sm,n}}{T}\right) \\ \times \exp\left\{ j\left(-\omega_T \tau_{sm,n} + \dfrac{\gamma_T}{2}\left(t' + u - \tau_{sm,n}\right)^2 \right) \right\} \end{array}\right] du , \tag{59}$$

which may be simplified to

$$y(t',n) = A_R e^{-j\omega_T \tau_{sm,n}} \int_{-\infty}^{\infty} \text{rect}\left(\frac{u}{T}\right) \text{rect}\left(\frac{u + t' - \tau_{sm,n}}{T}\right) e^{-jq\frac{\gamma_T}{2}(u)^2} e^{j\frac{\gamma_T}{2}\left(u + t' - \tau_{sm,n}\right)^2} du, \quad (60)$$

and further simplified to

$$y(t',n) = A_R e^{\left[\begin{matrix} -j\omega_T \tau_{sm,n} \\ +j\frac{\gamma_T}{2}\left(t' - \tau_{sm,n}\right)^2 \end{matrix}\right]} \int_{-\infty}^{\infty} \text{rect}\left(\frac{u}{T}\right) \text{rect}\left(\frac{u + t' - \tau_{sm,n}}{T}\right) e^{j\frac{\gamma_T}{2}\left[\begin{matrix} (1-q)u^2 \\ +2\left(t' - \tau_{sm,n}\right)u \end{matrix}\right]} du. \quad (61)$$

Recall that $q \in \{-1, +1\}$. For the case when the echo and kernel have the same chirp-rate sign, namely when $q = +1$, then this reduces to

$$y(t',n) = A_R e^{\left[\begin{matrix} -j\omega_T \tau_{sm,n} \\ +j\frac{\gamma_T}{2}\left(t' - \tau_{sm,n}\right)^2 \end{matrix}\right]} \int_{-\infty}^{\infty} \text{rect}\left(\frac{u}{T}\right) \text{rect}\left(\frac{u + t' - \tau_{sm,n}}{T}\right) e^{j\gamma_T\left(t' - \tau_{sm,n}\right)u} du. \quad (62)$$

For the larger time-bandwidth products of interest to us, this may be calculated to be approximately

$$\begin{aligned} y(t',n) &\approx A_R e^{\left[\begin{matrix} -j\omega_T \tau_{sm,n} \\ +j\frac{\gamma_T}{2}\left(t' - \tau_{sm,n}\right)^2 \end{matrix}\right]} \int_{-T/2}^{T/2} e^{j\gamma_T\left(t' - \tau_{sm,n}\right)u} du \\ &\approx T A_R e^{\left[\begin{matrix} -j\omega_T \tau_{sm,n} \\ +j\frac{\gamma_T}{2}\left(t' - \tau_{sm,n}\right)^2 \end{matrix}\right]} \text{sinc}\left(\frac{\gamma_T}{2\pi} T\left(t' - \tau_{sm,n}\right)\right), \qquad \text{for } q = +1. \end{aligned} \quad (63)$$

This is the continuous-time equivalent to Eq. (27), and exhibits the expected sinc function behavior of the mainlobe.

For the case when the echo and kernel have a different chirp-rate sign, namely when $q = -1$, then Eq. (61) becomes

$$y(t',n) = A_R e^{\left[\begin{matrix} -j\omega_T \tau_{sm,n} \\ +j\frac{\gamma_T}{2}\left(t' - \tau_{sm,n}\right)^2 \end{matrix}\right]} \int_{-\infty}^{\infty} \text{rect}\left(\frac{u}{T}\right) \text{rect}\left(\frac{u + t' - \tau_{sm,n}}{T}\right) e^{j\gamma_T\left[u^2 + \left(t' - \tau_{sm,n}\right)u\right]} du. \quad (64)$$

Note that now the integrand is itself a chirp. Note also that the correlation kernel is simply the complex conjugate of the correct one.

We may transmogrify this to

$$y(t',n) = A_R e^{\left[\begin{matrix}-j\omega_T\tau_{sm,n} \\ +j\frac{\gamma_T}{4}\left(t'-\tau_{sm,n}\right)^2\end{matrix}\right]} \int_{-\infty}^{\infty} \text{rect}\left(\frac{u}{T}\right)\text{rect}\left(\frac{u+t'-\tau_{sm,n}}{T}\right) e^{j\gamma_T\left(u+\frac{t'-\tau_{sm,n}}{2}\right)^2} du\,. \qquad (65)$$

Note that the phase of the integrand has a stationary point well within the limits of the rect function. This implies that we can ignore the limits of the rect functions and calculate

$$y(t',n) \approx \sqrt{\frac{\pi}{\gamma_T}} A_R e^{j\left[\frac{\pi}{4}-\omega_T\tau_{sm,n}+\frac{\gamma_T}{4}\left(t'-\tau_{sm,n}\right)^2\right]}, \quad \text{for } q=-1\,. \qquad (66)$$

To put some perspective on a comparison of this to Eq. (63), let us consider a 500 MHz chirp over a 20 μs pulsewidth. For this example, the ratio of the sinc function peak in Eq. (63) to the integrated floor of Eq. (66) yields

$$\frac{T}{\sqrt{\frac{\pi}{\gamma_T}}} \approx 141, \text{ or approximately 43 dB.} \qquad (67)$$

This would be the additional attenuation of, say, an ambiguous range return for a wrong chirp-rate sign for this example waveform.

A Note about Stretch Processing

While the above development was for correlation processing, we observe that stretch processing is also an approximation to correlation processing, hence processing wrong-sign chirps will be limited by Eq. (66) as well. In fact, the reduction may be even greater.

Recall that the first step in stretch processing is to deramp the chirp, accomplished by mixing (multiplying) the echo signals with a reference chirp. However, if the echo chirps have the wrong sign, instead of dechirping the echoes, we will instead be doubling their chirp-rate. After mixing, the (intended to be) dechirped signal is filtered usually to a substantially less Intermediate Frequency (IF) and video bandwidth. Consequently, an echo for which the chirp rate has been doubled will find only a small fraction of its bandwidth fitting through the subsequent IF and video filters. For a chirp, bandwidth is proportional to energy.

The result is that for stretch processing, we may witness that the net energy passed by the IF and video filters for a wrong-sign chirp may be reduced by up to several tens of additional dB.

“One picture is worth 1,000 denials.”
-- Ronald Reagan

4 Coherently Combining Up and Down Chirps

The question now becomes "If we have a CPI, or synthetic aperture, that contains echoes from both up-chirps and down-chirps, how do we coherently combine them? How do we compensate one to match the other?"

4.1 Output of Correlation Processing

Recall that for correlation processing

$$\begin{aligned} Y(u,n) &\approx KA_R \operatorname{sinc}\left(\frac{\gamma_T}{2\pi} T_s K\left(T_s u - \tau_{sm,n}\right)\right) e^{-j\omega_T \tau_{sm,n}} e^{jq\frac{\gamma_T}{2}\left[\left(T_s u-\tau_{sm,n}\right)^2 - \left(T_s u-\tau_{sm,n}\right)T_s\right]} \\ &\approx KA_R \operatorname{sinc}\left(\frac{\gamma_T}{2\pi} T_s K\left(T_s u - \tau_{sm,n}\right)\right) e^{-j\omega_T \tau_{sm,n}} . \end{aligned} \tag{68}$$

After range compression, the sign of the chirp-rate q has only a very minor, in fact typically negligible, role to play. Consequently, no further processing is required to reconcile up-chirps with down-chirps.

Example

We exemplify this section by implementing a simulation of alternating up-chirps and down-chirps with each pulse during a CPI using Eq. (19) with range-compression correlation kernel of Eq. (21), except that a Hamming window taper function was employed to reduce processing sidelobes.[8] The result is then further processed with a DFT across the pulses, also with a Hamming window taper function, to yield the Impulse Response (IPR) in Figure 3. The Hamming windows were employed to reduce processing sidelobes, and help reveal effects of any residual signal modulations due to the alternating up/down chirps.

The parameters used in this example include

$$\begin{aligned} &\omega_T = 2\pi\, 16.7\times 10^9 \text{ rad/s}, \\ &B_c = 500 \text{ MHz}, \\ &T = 20 \text{ μs}, \\ &T_s = 0.5 \text{ ns}, \\ &T_L = 20.2 \text{ μs, and} \\ &N = 512 \text{ pulses}. \end{aligned} \tag{69}$$

In addition, the point echo response was created at a zero range offset, but changing at a rate of 10 cycles of phase over the CPI.

We observe no unusual sidelobes in Doppler (or range) due to the alternating chirp-rate sign. This anecdotal evidence supports the simplification of the correlation processing output model to the second line of Eq. (68).

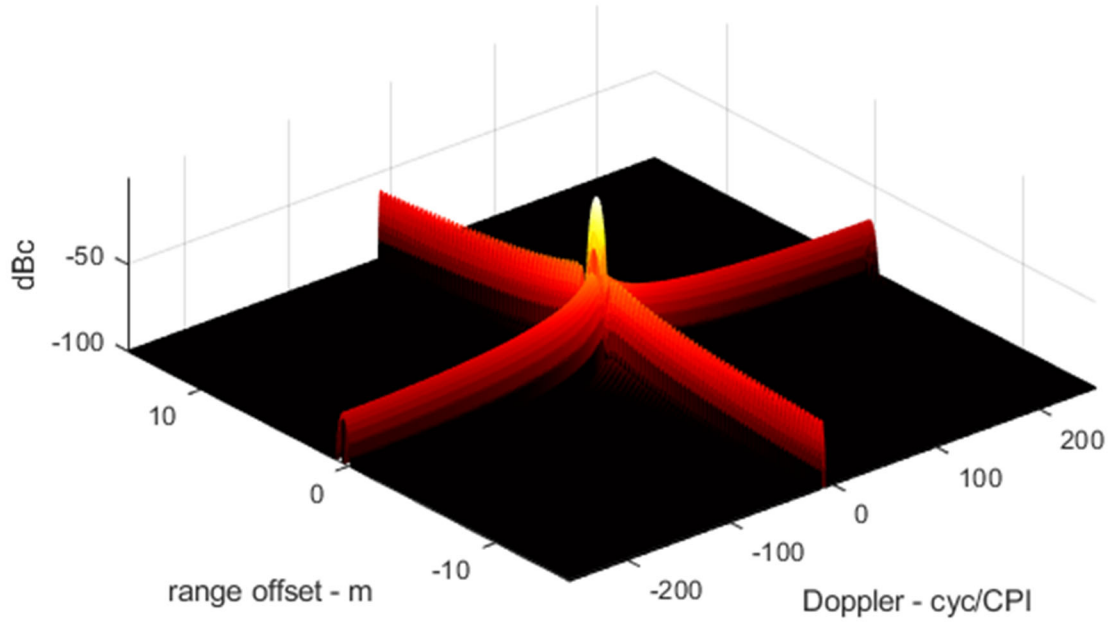

Figure 3. Example IPR of CPI using alternating up-chirp and down-chirp, using correlation processing.

4.2 Output of Stretch Processing

Recall that for stretch processing

$$Y(u,n) \approx IA_R \operatorname{sinc}\left(\frac{\gamma_T}{2\pi}T_s I\left(\frac{qu}{\frac{\gamma_T}{2\pi}T_s I}+\tau_{sm,n}\right)\right)e^{-j\omega_T\tau_{sm,n}}e^{jq\frac{\gamma_T}{2}\tau_{sm,n}^{\ 2}}. \tag{70}$$

As previously discussed, after range compression, the sign of the chirp-rate q appears twice with significant impact. The intent is to process the range-compressed data modelled in Eq. (70) to a form that is independent of chirp-rate sign q. This necessitates two principal actions,

1. Dealing with the index direction inside the sinc function, and
2. Dealing with the RVPE term.

The compensation for these can be done in either order, but we will take them in the order given.

Index Reversal

Let us define a new index as follows

$$u' = -qu\,. \tag{71}$$

Therefore, re-indexing in this manner yields

$$Y'\left(u',n\right) \approx IA_R \operatorname{sinc}\left(\frac{\gamma_T}{2\pi}T_s I\left(\frac{-u'}{\frac{\gamma_T}{2\pi}T_s I}+\tau_{sm,n}\right)\right)e^{-j\omega_T\tau_{sm,n}}e^{jq\frac{\gamma_T}{2}\tau_{sm,n}^{\,2}}, \tag{72}$$

which, because the sinc function is even, may also be written as

$$Y'\left(u',n\right) \approx IA_R \operatorname{sinc}\left(\frac{\gamma_T}{2\pi}T_s I\left(\frac{u'}{\frac{\gamma_T}{2\pi}T_s I}-\tau_{sm,n}\right)\right)e^{-j\omega_T\tau_{sm,n}}e^{jq\frac{\gamma_T}{2}\tau_{sm,n}^{\,2}}. \tag{73}$$

The indexing direction is now consistent for all q.

RVPE Compensation

We now compensate for the RVPE term by multiplying

$$Y''\left(u',n\right) \approx Y'\left(u',n\right)e^{-jq\frac{\gamma_T}{2}\hat{\tau}_{sm,n}^{\,2}}, \tag{74}$$

where we estimate for each index value u'

$$\hat{\tau}_{sm,n} = \frac{u'}{\frac{\gamma_T}{2\pi}T_s I} = \frac{u'}{B_{eff}}. \tag{75}$$

Doing so yields

$$Y''\left(u',n\right) \approx IA_R \operatorname{sinc}\left(\frac{\gamma_T}{2\pi}T_s I\left(\frac{u'}{\frac{\gamma_T}{2\pi}T_s I}-\tau_{sm,n}\right)\right)e^{-j\omega_T\tau_{sm,n}}\,. \tag{76}$$

With the RVPE thus compensated, albeit with an approximation, no further dependence on chirp-rate sign is evident, and pulses originating with different q can be coherently combined.

Example

We exemplify this section by implementing a simulation of alternating up-chirps and down-chirps with each pulse during a CPI using Eq. (44) with range-compression processing as expressed in Eq. (45), except that a Hamming window taper function was employed to reduce processing sidelobes.[8]

Subsequently, the re-indexing of Eq. (71), and the RVPE correction of Eq. (74), have been applied. The result is then further processed with a DFT across the pulses, also with a Hamming window taper function, to yield the Impulse Response (IPR) in Figure 4. As with correlation processing, the Hamming windows were employed to reduce processing sidelobes, and help reveal effects of any residual signal modulations due to the alternating up/down chirps.

The parameters used in this example include

$$\begin{aligned} &\omega_T = 2\pi\, 16.7\times 10^9 \text{ rad/s,} \\ &B_c = 500 \text{ MHz,} \\ &T_s = 80 \text{ ns,} \\ &T_L = 20 \text{ μs, and} \\ &N = 512 \text{ pulses.} \end{aligned} \tag{77}$$

In addition, the point echo response was created at 3 m nearer than the center reference range, but changing at a rate of 10 cycles of phase over the CPI.

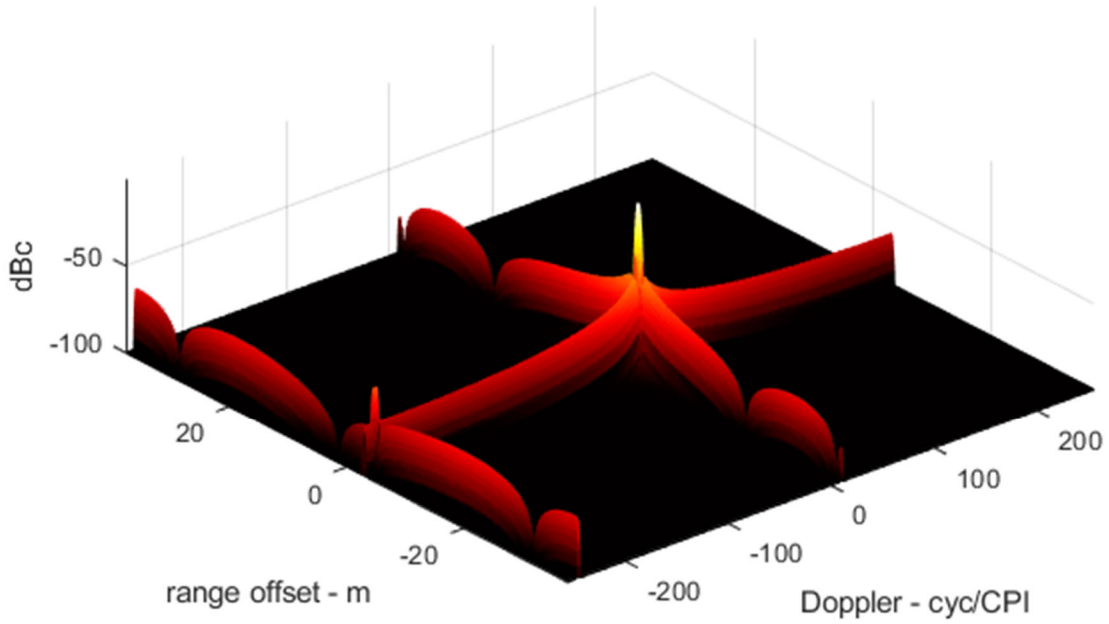

Figure 4. Example IPR of CPI using alternating up-chirp and down-chirp, using stretch processing.

We note that a −50 dBc processing anomaly exists at about −246 cycles/CPI, corresponding to half the sampling frequency offset from the principal IPR peak. This is an artifact due to the RVPE correction of Eq. (74) using an estimate Eq. (75) appropriate for the center of the range bin. Any echo range not exactly in the center of the range bin will have a residual error that is modulated by changes in q. Since our example has q alternating on every pulse, the error will be offset by half the sampling frequency, as is evident in Figure 4.

Note that any echo that exhibits range migration will in fact not remain static in the center of a range bin, or in any other part of a range bin.

Some Comments on DFT Processing of the De-Ramped Echo Signals

Coherently combining two pulses, especially two pulses with different chirp-rate signs, requires the following

1. Both pulses chirp over exactly the same frequency band, and
2. Both pulses are processed to exactly the same range swath.

This requires us to pay close attention to our index definitions.

Recall that our echo return model is given in Eq. (43), repeated here as

$$X_V(i,n) = A_R \exp\left\{ j\left(-\omega_T \tau_{sm,n} - \; q\gamma_T \tau_{sm,n} T_s i \; + \; q\frac{\gamma_T}{2}{\tau_{sm,n}}^2 \right) \right\}. \tag{78}$$

To the first point, that both pulses chirp over exactly the same frequency band, this requires that there is a one-to-one correspondence between positive index i and negative index i. In the earlier development, we assumed that there were an odd number I of fast-time samples collected, and that the index took on integer values such that

$$-(I-1)/2 \;\le\; i \;\le\; (I-1)/2, \text{ for odd } I. \tag{79}$$

In this case, the center integer index $i = 0$ corresponds to the reference center time of the data vector. With these definitions, our criterion is met.

If the number of fast-time samples is to be even, that is I is even, then Eq. (79) still holds, except that index i is limited to 'half' values, that is integer offsets from $1/2$, but still incrementing in unit steps. These may be mapped to integer values of a different index such that

$$\begin{aligned} i \;&= i' + \frac{1}{2}, \text{ for integer } \; i' \text{ which means} \\ -I/2 \;&\le\; i' \;\le\; I/2 - 1, \text{ for even } I. \end{aligned} \tag{80}$$

The reference time, however, still needs to occur at $i = 0$, which for the new index now occurs at $i' = -1/2$. This needs to be accounted for in radar Timing and Control (T&C) equations.

With index *i* so defined, the DFT of Eq. (78) may still be so written as in Eq. (46), namely

$$Y(u,n) = A_R e^{-j\omega_T \tau_{sm,n}} e^{jq\frac{\gamma_T}{2}\tau_{sm,n}{}^2} \sum_{i=-(I-1)/2}^{(I-1)/2} e^{-jq\gamma_T \tau_{sm,n} T_s i} e^{-j2\pi\frac{u}{U}i} . \tag{81}$$

This worked fine for an odd *I*, and using Eq. (80), will also work fine for an even *I*. However, the result in Eq. (47) for an arbitrary *I*, but still an odd *U*, becomes now

$$Y(u,n) = IA_R \left(\frac{\sin\left(\pi \frac{I}{2\pi}\left(q\gamma_T \tau_{sm,n} T_s + 2\pi\frac{u}{U}\right)\right)}{I\sin\left(\pi \frac{1}{2\pi}\left(q\gamma_T \tau_{sm,n} T_s + 2\pi\frac{u}{U}\right)\right)} \right) e^{-j\omega_T \tau_{sm,n}} e^{jq\frac{\gamma_T}{2}\tau_{sm,n}{}^2} . \tag{82}$$

Note that this now allows $U \approx I$, but still assumes

$$-(U-1)/2 \le u \le (U-1)/2, \text{ for odd } U. \tag{83}$$

Now, to the second point, that both pulses are processed to exactly the same range swath. The fact that we need to perform an index reversal requires that there is a one-to-one correspondence between positive index *u* and negative index *u*. In the earlier development, we assumed that *U* was also an odd number, with the center index value $u = 0$ defining the nominal center of the range swath. With these definitions, our criterion is met.

However, if the number of output samples is to be even, that is *U* is even, then Eq. (82) still holds, except that index *u* is limited to 'half' values, that is integer offsets from $1/2$. These may be mapped to integer values of a different index such that

$$\begin{aligned} u &= u' + \frac{1}{2}, \text{ for integer } u' \text{ which means} \\ -U/2 &\le u' \le U/2 - 1, \text{ for even } U. \end{aligned} \tag{84}$$

In this case, the swath center is not at an integer index, but rather at $u' = -1/2$. i.e. between integer index values.

Nevertheless, while even values for fast-time samples and/or output swath complicate the processing somewhat, coherently combining up/down chirp data is still quite feasible.

5 Considering Intra-Pulse Doppler

The preceding development assumed the "stop-and-go" model for the echo return signal, where no relative target motion occurred during any individual pulse echo. i.e. between transmitting a signal and receiving its echo. We now examine the case of a constant relative velocity during the pulse echo.

We recall that we could model our return echo signal as Eq. (11). Using this and several parameter definitions and simplifications, Eq. (11) can be written as

$$X_V(i,n) = \left[\begin{array}{l} A_R \,\mathrm{rect}\left(\dfrac{T_s i - \tau_{sm,n}}{T} \right) \mathrm{rect}\left(\dfrac{T_s i}{T_L} \right) \\ \times \exp\left\{ j \left(\begin{array}{l} -\omega_T \tau_{sm,n} \\ +q \dfrac{\gamma_T}{2} \left(T_s i - \tau_{sm,n} \right)^2 - q \dfrac{\gamma_L}{2} \left(T_s i \right)^2 \end{array} \right) \right\} \end{array} \right]. \tag{85}$$

Now, to accommodate relative target motion during the pulse echo, we modify the relative pulse echo delay to

$$\tau_{sm,n} \to \tau_{sm,n} + \dot{\tau}_{sm,n} T_s i \,, \tag{86}$$

where

$$\dot{\tau}_{sm,n} = \text{the time-rate of change in the echo delay during the pulse echo.} \tag{87}$$

Combining Eq. (86) into Eq. (85), and rearranging a bit, yields

$$X_V(i,n) = \left[\begin{array}{l} A_R \,\mathrm{rect}\left(\dfrac{\left(1 - \dot{\tau}_{sm,n}\right) T_s i - \tau_{sm,n}}{T} \right) \mathrm{rect}\left(\dfrac{T_s i}{T_L} \right) \\ \times \exp\left\{ j \left(\begin{array}{l} -\omega_T \tau_{sm,n} - \omega_T \dot{\tau}_{sm,n} T_s i \\ +q \dfrac{\gamma_T}{2} \left(\left(1 - \dot{\tau}_{sm,n}\right) T_s i - \tau_{sm,n} \right)^2 - q \dfrac{\gamma_L}{2} \left(T_s i \right)^2 \end{array} \right) \right\} \end{array} \right]. \tag{88}$$

The inclusion of $\dot{\tau}_{sm,n}$ has two effects,

1. A slight frequency shift via the term $\omega_T \dot{\tau}_{sm,n} T_s i$, and

2. A slight compression or dilation of the timescale in the echo signal.

To put some context on the parameter $\dot{\tau}_{sm,n}$, we note that it may be calculated as

$$\dot{\tau}_{sm,n} = \frac{2}{c} v_{sm,n}, \tag{89}$$

where

$$v_{sm,n} = \text{the relative velocity of the target point with respect to the reference range.} \tag{90}$$

The velocity is a line-of-sight velocity.

Assuming a relative velocity of perhaps 100 m/s yields

1. For a Ku-band radar with a 20 μs pulse, a resulting 1.4 radians of phase shift over the pulse, and

2. A time compression factor $\left(1-\dot{\tau}_{sm,n}\right)$ of about $\left(1-6.67\times10^{-7}\right)$, or about 0.667 ppm.

This is pretty small.

Nevertheless, for typical airborne radar systems, the relative target motion of otherwise stationary clutter within the scene may be modelled with a bulk closing velocity and a much smaller variation across a neighborhood that the antenna beam illuminates. Moving ground vehicles also generally exhibit a slower relative velocity (with respect to stationary clutter), less than 100 m/s, and can often also be modelled as variations around a bulk closing velocity.

We state without elaboration that much of the effects of a bulk closing velocity can be mitigated by adjusting LO waveform parameters while collecting pulse echo data. These LO parameters might include phase, frequency, chirp rate, and even reference time. This is sometimes called real-time motion compensation. We will hereafter ignore this option.

5.1 Correlation Processing

Recall that this is the case where $\gamma_L = 0$, in which case Eq. (88) reduces to

$$X_V\left(i,n\right) = \left[\begin{array}{l} A_R \,\text{rect}\left(\dfrac{\left(1-\dot{\tau}_{sm,n}\right)T_s i - \tau_{sm,n}}{T}\right) \\ \times \exp\left\{ j\left(\begin{array}{l} -\omega_T \tau_{sm,n} - \omega_T \dot{\tau}_{sm,n} T_s i \\ +q\dfrac{\gamma_T}{2}\left(\left(1-\dot{\tau}_{sm,n}\right)T_s i - \tau_{sm,n}\right)^2 \end{array}\right)\right\} \end{array}\right]. \tag{91}$$

Assuming that a single bulk velocity suffices, then $\dot{\tau}_{sm,n}$ can be approximated with a constant, and the video signal can be corrected to

$$X'_V\left(i,n\right)=\left[\begin{array}{l} A_R e^{-j\omega_T \tau_{sm,n}} \\ \times \mathrm{rect}\left(\dfrac{\left(1-\dot{\tau}_{sm,n}\right)T_s i-\tau_{sm,n}}{T}\right) e^{jq\frac{\gamma_T}{2}\left(\left(1-\dot{\tau}_{sm,n}\right)T_s i-\tau_{sm,n}\right)^2} \end{array}\right]. \tag{92}$$

This is equivalent to Eq. (19) except that fast-time sample period T_s is now scaled by a presumed to be adequately constant $\left(1-\dot{\tau}_{sm,n}\right)$, which is for many cases less than about 1 ppm. While it might often be reasonably ignored, it can also easily be incorporated into the correlation kernel if desired. In any case, intra-pulse Doppler adds no new artifacts due to alternating up/down chirps.

5.2 Stretch Processing

Recall that this is the case where $\gamma_L=\gamma_T$, in which case Eq. (88) reduces to

$$X_V\left(i,n\right)=A_R\exp\left\{j\left(\begin{array}{l} -\omega_T\tau_{sm,n}-q\gamma_T\left(\tau_{sm,n}\right)\left(1-\dot{\tau}_{sm,n}\right)\left(T_s i\right)+q\dfrac{\gamma_T}{2}\left(\tau_{sm,n}\right)^2 \\ -\omega_T\dot{\tau}_{sm,n}T_s i-q\gamma_T\left(\dot{\tau}_{sm,n}-\dfrac{\dot{\tau}_{sm,n}{}^2}{2}\right)\left(T_s i\right)^2 \end{array}\right)\right\}. \tag{93}$$

Assuming that a single bulk velocity suffices, then $\dot{\tau}_{sm,n}$ can be approximated with a constant, and the video signal can be corrected to

$$X'_V\left(i,n\right)=A_R\exp\left\{j\left(-\omega_T\tau_{sm,n}-q\gamma_T\tau_{sm,n}\left(1-\dot{\tau}_{sm,n}\right)T_s i+q\frac{\gamma_T}{2}\tau_{sm,n}{}^2\right)\right\}. \tag{94}$$

This is equivalent to Eq. (43) except that fast-time sample period T_s is now scaled by a presumed to be adequately constant $\left(1-\dot{\tau}_{sm,n}\right)$, which is for many cases less than about 1 ppm. While it might often be reasonably ignored, it can also easily be accommodated as a scale factor to $\tau_{sm,n}$ if desired. In any case, intra-pulse Doppler adds no new artifacts due to alternating up/down chirps.

“I'm positive about the negative, but a little negative about the positive.”
-- Curly Howard

6 Conclusions

We offer and repeat some key points.

- Coherently combining up-chirps with down-chirps requires careful attention to ensure that echo signals have the same frequency content, and cover the same range swath.
- Up/down LFM chirps are relatively easy to combine when correlation processing is used.
- Up/down LFM chirps are somewhat more challenging to combine when stretch processing is used.
    - Some finer points to the DFT need to be considered to maintain coherence.
    - In addition, limits to the accuracy and precision with which the Residual Video Phase Error can be compensated result in unavoidable residual artifacts in the range-Doppler image or map.
- High-performance radar systems that need to consider intra-pulse Doppler can also be straightforwardly accommodated.

Figure 5. Musical symbols for "Portamento," a continuous glide from one pitch to another, a.k.a. an LFM chirp.

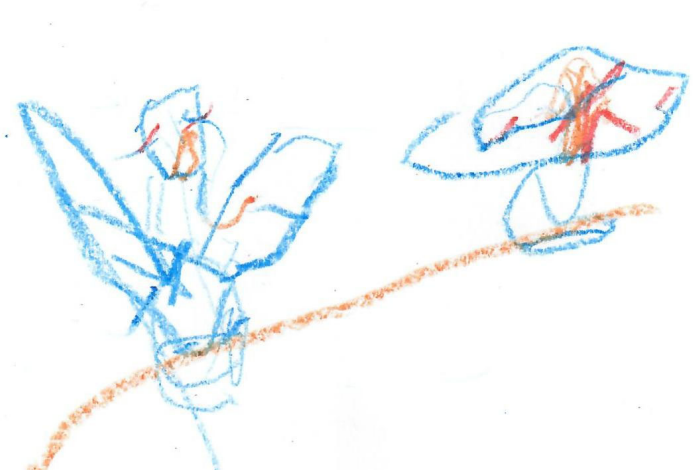

Figure 6. Two birds chirping (courtesy Gavin Spaulding, 3)

Appendix A – Examination of the Discrete Fourier Transform

The Discrete Fourier Transform (DFT) is a calculation of a sampled frequency response from sampled data. Strictly speaking, a frequency response is calculated from temporal data. However, we may equivalently calculate wavenumber response from spatial data or any harmonic components from data sampled in any domain.

One customary formulation of the DFT is

$$G(v) = \sum_{k=0}^{K-1} g(k) e^{-j2\pi \frac{v}{K} k}, \text{ for } 0 \le v \le K-1. \tag{A1}$$

Likewise, the inverse transform is customarily calculated as

$$g(k) = \frac{1}{K} \sum_{v=0}^{V-1} G(v) e^{+j2\pi \frac{k}{K} v}, \text{ for } 0 \le k \le K-1. \tag{A2}$$

Eq. (A1) is often called the forward transform, and Eq. (A2) is often called the inverse transform, e.g. the Inverse-DFT (IDFT). Other formulations also exist, and are no less valid representations.

The sampled nature of the data and spectrum stipulates a replication characteristic where

$$\begin{aligned} &G(v \pm K) = G(v), \text{ and} \\ &g(k \pm K) = g(k). \end{aligned} \tag{A3}$$

Note that we can calculate the DFT at other output spacings by formulating

$$G(v) = \sum_{k=0}^{K-1} g(k) e^{-j2\pi \frac{v}{V} k}, \text{ for } 0 \le v \le V-1. \tag{A4}$$

In this case, the spectrum is repeated as

$$G(v \pm V) = G(v). \tag{A5}$$

This is equivalent to having the input data zero-padded to a length V to achieve a finer frequency spacing in the DFT output.

Note that these definitions assume the underlying indices begin at an index value of zero, and end at $(K-1)$ or $(V-1)$. There is no inherent requirement for vector lengths to be even or odd in length, although certain values lend themselves better to fast techniques, in which case the DFT is referred to as a Fast Fourier Transform (FFT). In practice, inconvenient-sized input data

lengths are often zero-padded to something more convenient for FFT algorithm implementations to facilitate processing time advantages.

Nevertheless, sometimes other indexing definitions offer advantage for algorithm analysis and development. This was the case in this report with Eq. (45). More generally, for Eq. (45) and Eq. (81), we required an input index to be symmetric about the center reference sample, and the output index to be symmetric about the DC frequency. A DFT so constrained might be written as

$$G\left(v-\frac{K-1}{2}\right)=\sum_{k=0}^{K-1} g\left(k-\frac{K-1}{2}\right)e^{-j\frac{2\pi}{K}\left(v-\frac{K-1}{2}\right)\left(k-\frac{K-1}{2}\right)},$$

$$\text{for } 0\le k\le K-1, \text{ and } 0\le v\le K-1. \tag{A6}$$

Note that for this formulation

$$g\left(-\frac{K-1}{2}\right) = \text{first sample of g( )},$$
$$g\left(+\frac{K-1}{2}\right) = \text{last sample of g( )},$$
$$G\left(-\frac{K-1}{2}\right) = \text{most negative frequency sample of G( ), and}$$
$$G\left(+\frac{K-1}{2}\right) = \text{most positive frequency sample of G( ).} \tag{A7}$$

Note that Eq. (A6) is equivalent to

$$G(v')=\sum_{k'=-(K-1)/2}^{(K-1)/2} g(k')e^{-j\frac{2\pi}{K}v'k'},$$

$$\text{for } -(K-1)/2\le k'\le (K-1)/2, \text{ and } -(K-1)/2\le v'\le (K-1)/2, \tag{A8}$$

where

$$k' = k-(K-1)/2, \text{ and}$$
$$v' = v-(K-1)/2. \tag{A9}$$

Note also that for even vector lengths, respective indices might take on half values, that is integer offsets from $1/2$, but still incrementing in unit steps.

Nevertheless, Eq. (A6) can be expanded to

$$G\left(v-\frac{K-1}{2}\right)=e^{j\frac{2\pi}{K}\left(\frac{K-1}{2}\right)\left(v-\frac{K-1}{2}\right)}\sum_{k=0}^{K-1}\left[g\left(k-\frac{K-1}{2}\right)e^{j\frac{2\pi}{K}\left(\frac{K-1}{2}\right)k}\right]e^{-j\frac{2\pi}{K}vk}. \tag{A10}$$

So, to implement the DFT as defined in Eq. (A8), we may use the customary definition in Eq. (A1), with some additional processing steps, namely

1. Pre-multiplying $g\left(k-\frac{K-1}{2}\right)$ with $e^{j\frac{2\pi}{K}\left(\frac{K-1}{2}\right)k}$,
2. Performing the customary DFT as defined in Eq. (A1), and
3. Post-multiplying the result by $e^{j\frac{2\pi}{K}\left(\frac{K-1}{2}\right)\left(v-\frac{K-1}{2}\right)}$.

The result is that

$$G\left(v'\right)=G\left(v-\frac{K-1}{2}\right). \tag{A11}$$

In this manner, we can use conventional DFT tools and definitions to implement the more convenient architectures used in this report.

“Everything should be made as simple as possible, but not simpler.”
-- Albert Einstein

Reference

[1] John R. Klauder, A. C. Price, Sidney Darlington, Walter J. Albersheim, "The theory and design of chirp radars," *Bell System Technical Journal*, Vol. 39, No. 4, pp. 745-808, 1960.

[2] A. W. Doerry, J. M. Andrews, S. M. Buskirk, "Digital synthesis of linear-FM chirp waveforms – comments on performance and enhancements," SPIE 2014 Defense & Security Symposium, Radar Sensor Technology XVIII, Vol. 9077, Baltimore MD, 5–9 May 2014.

[3] Josef Mittermayer, José Márquez Martínez, "Analysis of range ambiguity suppression in SAR by up and down chirp modulation for point and distributed targets," *Proceedings of the 2003 IEEE International Geoscience and Remote Sensing Symposium*, IGARSS 2003, Vol. 6, pp. 4077-4079, 2003.

[4] Wen-Qin Wang, "MIMO SAR chirp modulation diversity waveform design," *IEEE Geoscience and Remote Sensing Letters*, Vol. 11, No. 9, pp. 1644-1648, 2014.

[5] Amro Lulu, Bijan G. Mobasseri, "Chirp diversity waveform design and detection by stretch processing," *Proceedings of the 2016 IEEE Radar Conference (RadarConf)*, pp. 1-6, 2016.

[6] William J. Caputi, Jr., "Stretch: A Time-Transformation Technique", *IEEE Transactions on Aerospace and Electronic Systems*, Vol. AES-7, No. 2, pp 269-278, March 1971.

[7] Armin W. Doerry, *Digital Signal Processing of Radar Pulse Echoes*, Sandia National Laboratories Report SAND2020-9428, Unlimited Release, September 2020.

[8] Armin W. Doerry, *Catalog of Window Taper Functions for Sidelobe Control*, Sandia National Laboratories Report SAND2017-4042, Unlimited Release, April 2017.

Distribution

Unlimited Release

Email—External

Brandeis Marquette	Brandeis.Marquette@ga-asi.com	General Atomics ASI
Jean Valentine	Jean.Valentine@ga-asi.com	General Atomics ASI
John Fanelle	John.Fanelle@ga-asi.com	General Atomics ASI

Email—Internal

all members	534x	
Technical Library	9536	libref@sandia.gov

Sandia National Laboratories is a multimission laboratory managed and operated by National Technology & Engineering Solutions of Sandia LLC, a wholly owned subsidiary of Honeywell International Inc. for the U.S. Department of Energy's National Nuclear Security Administration under contract DE-NA0003525.